Preprints (www.preprints.org) | NOT PEER-REVIEWED | Posted: 3 June 2022 doi:10.20944/preprints202206.0049.v1

Type of the Paper (Tutorial)

A Semi-Synthetic Study of Multidimensional Imaging using a Scattering Lens

Shivasubramanian Gopinath[1]

1. PG and Research Department of Physics, Thiagarajar College, Madurai, Tamil Nadu, India; gopishiva62@gmail.com

Abstract: Scattering has been always considered a problem in most of the imaging and holography systems. In this project, a 3D imaging system has been developed based on scattering against common beliefs. The 3D imaging system consists of only two components namely a scattering lens, fabricated by grinding the surface of a convex lens using sandpaper and a web camera. The point spread function (PSF) in the form of speckle distribution was recorded using a laser source in the first step. A synthetic object was selected which was convolved with the PSF in a computer to generate the object intensity distribution. The image of the object was reconstructed by processing the PSF and object intensity distribution using a computational reconstruction method called non-linear reconstruction. The recorded PSF was scaled and the process was repeated for a different synthetic object. The concept was extended to 3D by summing the object intensity distributions generated using PSFs with different scaling factors. The image at different planes can be reconstructed using the PSFs corresponding to that plane.

Keywords: : Computational Imaging, Non-linear reconstruction (NLR), Holography, scattering lens, 3D imaging.

1. Introduction

In the past, imaging systems depended only on the optical modulator. This dependency affected imaging technology adversely causing a heavy load on the manufacturing processes increasing the cost of imaging systems. The developments in signal processing and computers extended the dependency on imaging reducing the demand for manufacturing and expanding the imaging capabilities. In this interdisciplinary area, computational imaging stands on three pillars namely optics, signal processing, and computer, which is the future of imaging [1-4]. Computational imaging methods can also overcome physical limitations in imaging systems such as sensing color using monochrome sensors and depth using 2D cameras [5-8]. Computational imaging serves a broad range of scientific, defense, and biomedical applications [9,10].

Initial reports on computational imaging using x-rays and gamma rays emerged in 1968 [11, 12]. With developments in signal processing methods, the computational imaging methods were widely used [13-15]. Most of the recently reported computational imaging methods either used an active optical modulator such as a spatial light modulator or elements fabricated using advanced manufacturing methods [16-20]. The above requirements root from the fact that multiple camera shots or an engineered intensity and phase distribution were needed. As a result, the cost of computational imaging methods is high.

In this project, a cost-effective computational imaging method has been developed. Instead of a scientific camera, a low-cost web camera valued at ~600 INR (~8 USD) was used. Instead of an SLM or a quasi-random lens manufactured using

Preprints (www.preprints.org) | NOT PEER-REVIEWED | Posted: 3 June 2022 doi:10.20944/preprints202206.0049.v1

advanced manufacturing methods, a refractive lens valued at ~80 INR (~1 USD) was used. The refractive lens was grinded using sandpaper to convert it into a scattering lens. The point spread functions (PSFs) were recorded using a laser and the object intensity patterns were synthesized in the computer using synthetic objects and recorded PSFs. Both 2D as well as 3D computational optical experiments were carried out.

2. Methods and Experiments

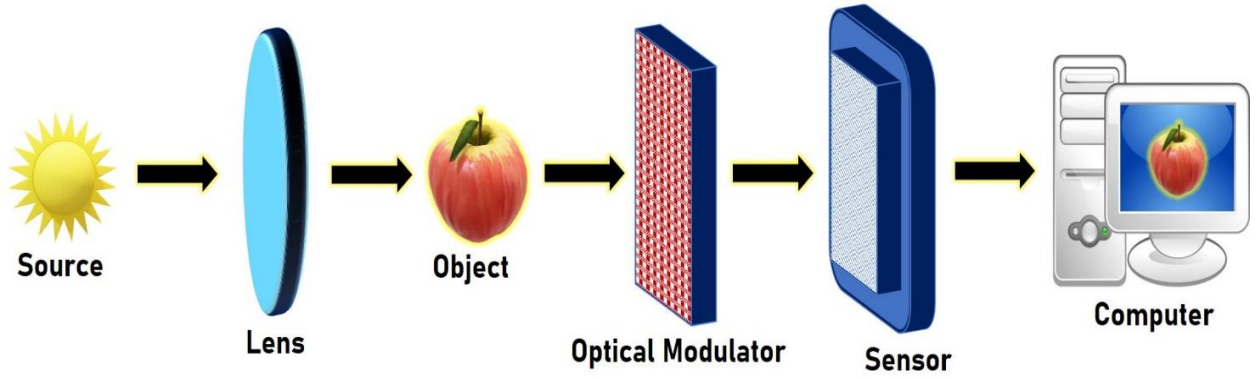

Figure 1 Optical configuration of a computational imaging system

The optical configuration of a computational imaging system is shown in Figure 1. An object is illuminated by a light source and the light diffracted from the object was modulated by an optical modulator which was collected by an image sensor. In this project, the optical modulator is a scattering lens and the sensor is a web camera. Unlike regular imaging where the image of the object is formed on the sensor, in computational imaging, the scattered intensity pattern is recorded by the sensor and reconstructed into the object information. The object intensity is $O=o\otimes PSF$, where o is the object function. The reconstruction is carried out by correlating O and PSF as $o'=O*PSF$. Instead of the noisy regular correlation, in this project, non-linear reconstruction was applied [15]. The non-linear reconstruction involved raising the magnitudes of the spectrum of PSF and O in powers of α and β and varying them between -1 to 1 until the least entropy was obtained. A refractive lens with a focal length of 10 cm was selected for the experiment. It was manually grinded using P-60 and P-280 sandpaper along all directions such that a uniform scattering can be achieved. The grinding process consumed 5 minutes per lens. The pictures of the front sides of the two grinded lenses P-60 and P-280 are shown in Figures 2 and 3 respectively. To have a reliable comparison, two glass plates with a thickness of approximately 2 mm were grinded using the same sandpapers P-60 and P-280. The pictures of the front surfaces of the two glass plates for P-60 and P-280 are shown in Figures 4 and 5 respectively.

Preprints (www.preprints.org) | NOT PEER-REVIEWED | Posted: 3 June 2022 doi:10.20944/preprints202206.0049.v1

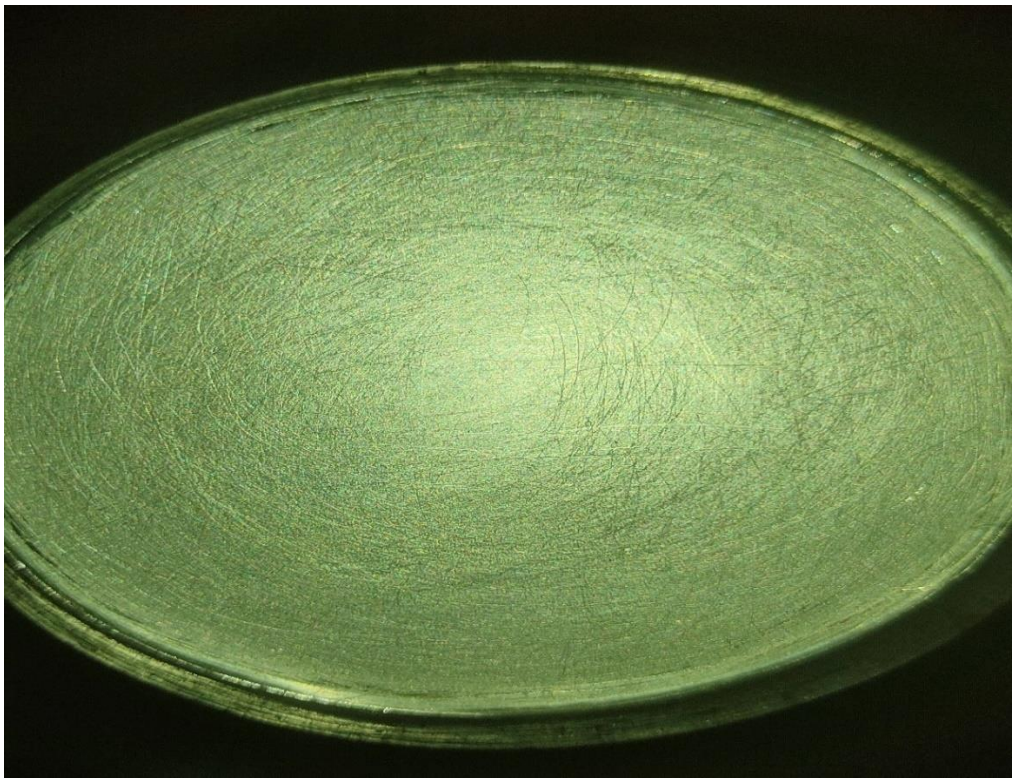

Figure 2 Lens grinded using P-60 sandpaper

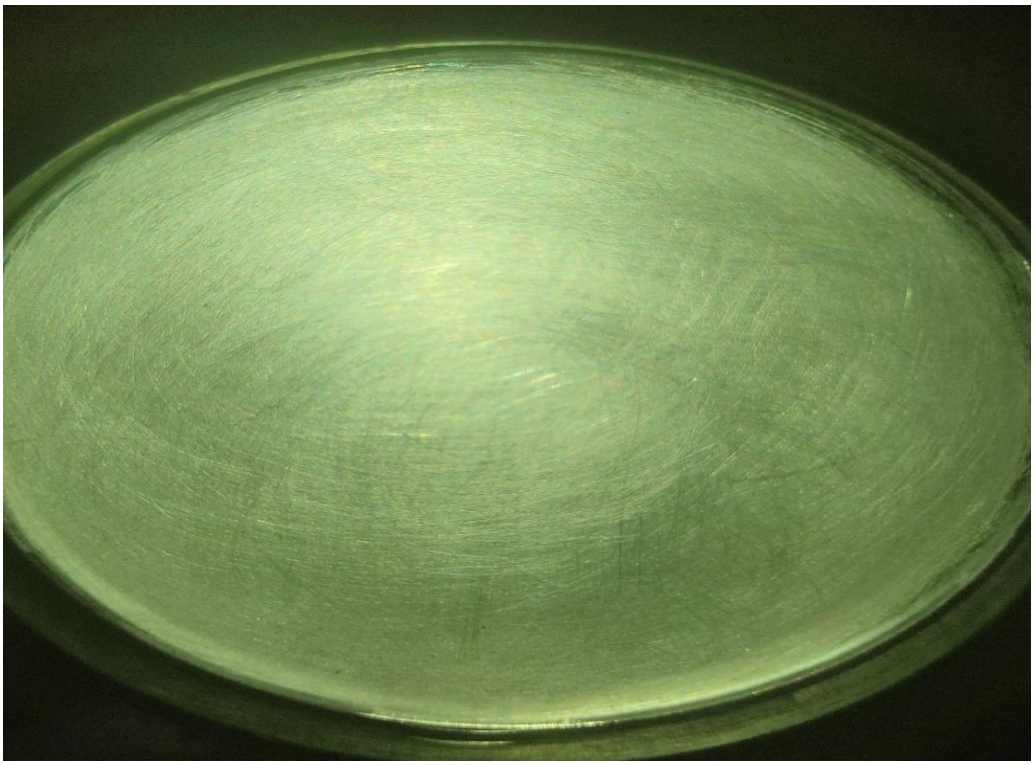

Figure 3 Lens grinded using P-280 sandpaper

Preprints (www.preprints.org) | NOT PEER-REVIEWED | Posted: 3 June 2022 doi:10.20944/preprints202206.0049.v1

Figure 4 Glass plate grinded using P-60 sandpaper

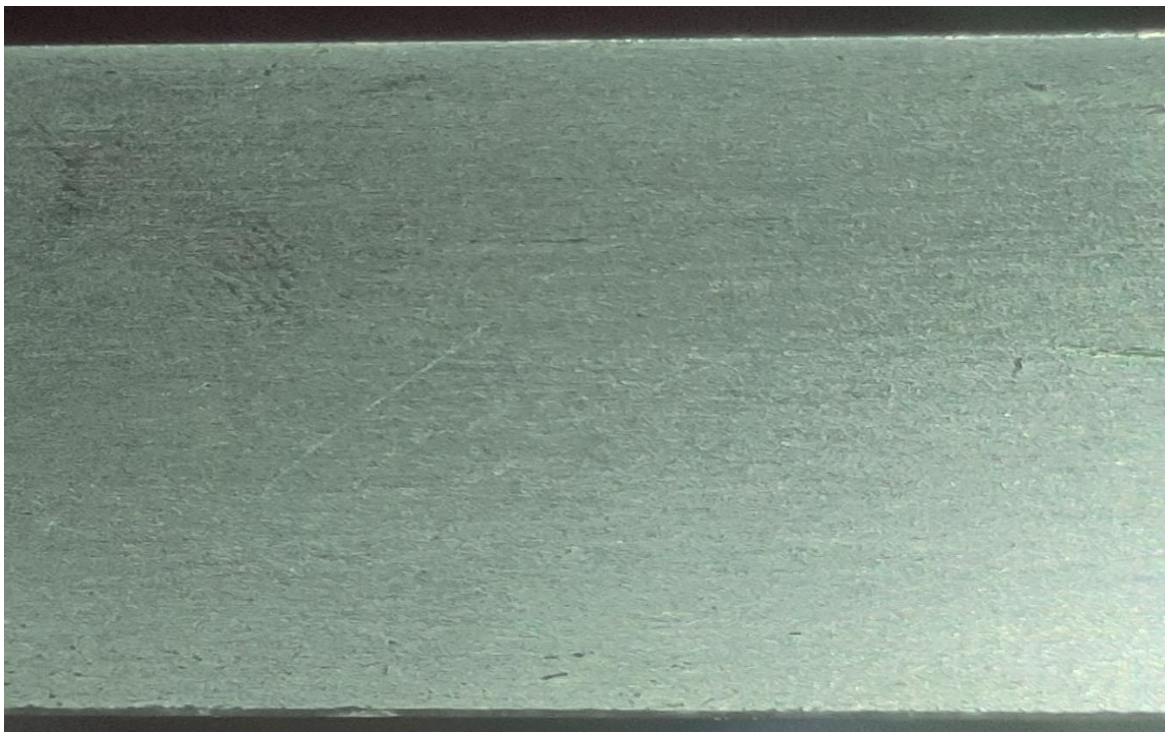

Figure 5 Glass plate grinded using P-280 sandpaper

The experimental setup is shown in Fig. 6. Light from a He-Ne Laser (632.8 nm) was collimated using a refractive lens and the collimated light was incident on the scattering lens. The scattered intensity distribution was captured by a web

Preprints (www.preprints.org) | NOT PEER-REVIEWED | Posted: 3 June 2022 doi:10.20944/preprints202206.0049.v1

camera [Quantum QHM495LM]. The images of the speckle distributions recorded for scattering lens (P-60), scattering lens (P-280), glass plate (P-60) and glass plate (P-280) are shown in Figures 7-10 respectively. As seen from the figures, with a lens, the speckle density was higher and the speckle sizes smaller than glass plates.

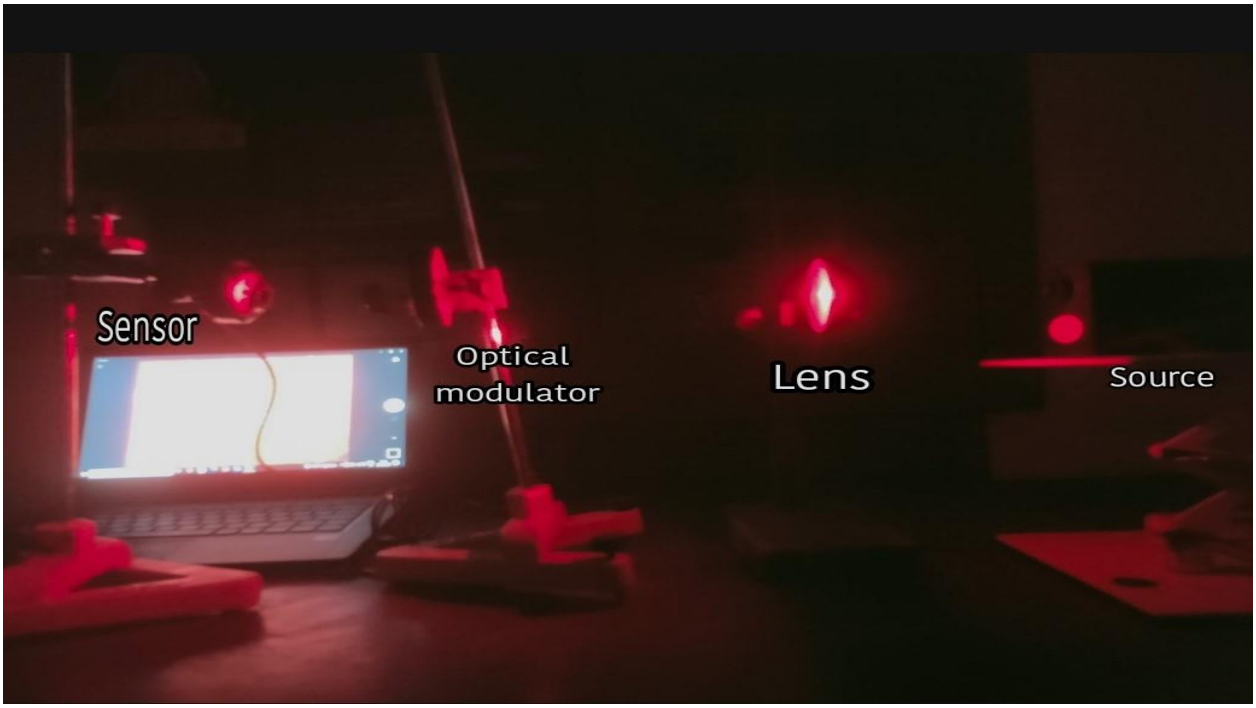

Figure 6 Experimental setup for recording the PSFs

Figure 7 Speckle pattern recorded for lens (P-60)

Preprints (www.preprints.org) | NOT PEER-REVIEWED | Posted: 3 June 2022 doi:10.20944/preprints202206.0049.v1

Figure 8 Speckle pattern recorded for lens (P-60)

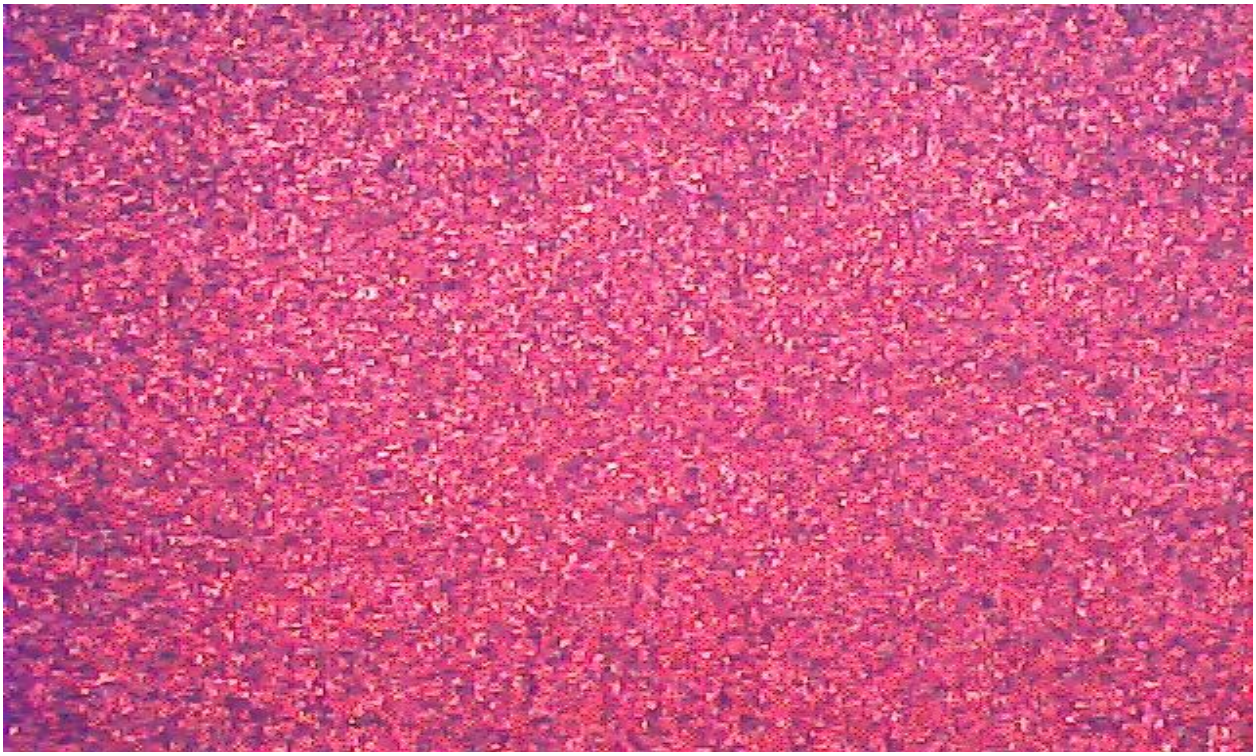

Figure 9 Speckle pattern recorded for glass plate (P-60)

Preprints (www.preprints.org) | NOT PEER-REVIEWED | Posted: 3 June 2022 doi:10.20944/preprints202206.0049.v1

Figure 10 Speckle pattern recorded for lens (P-280)

Two synthetic objects "smiley ball" and "cricket ball" were used for the demonstration of multidimensional imaging. The entire simulation was carried out using one recorded PSF. A second PSF was generated by scaling the recorded PSF by a factor 0.98. The images of the two PSFs are shown in Figures 11(a) and 11(b) respectively. The images of the two objects are shown in Figures 11(c) and 11(d) respectively. The first PSF was convolved with the smiley synthetic object to generate the object intensity pattern as shown in Figure 11(e). The second PSF is convolved with the second object and the generated intensity pattern is shown in Figure 11(f). The hologram containing two plane information obtained by summing 11(e) and 11(f) is shown in Figure 11(g). The reconstruction results for the two objects using the two PSFs are shown in Figures 11(h) and 11(i) respectively. As seen in Figures 11(h) and 11(i), only one of the objects appear focused while the other is blurred.

Preprints (www.preprints.org) | NOT PEER-REVIEWED | Posted: 3 June 2022 doi:10.20944/preprints202206.0049.v1

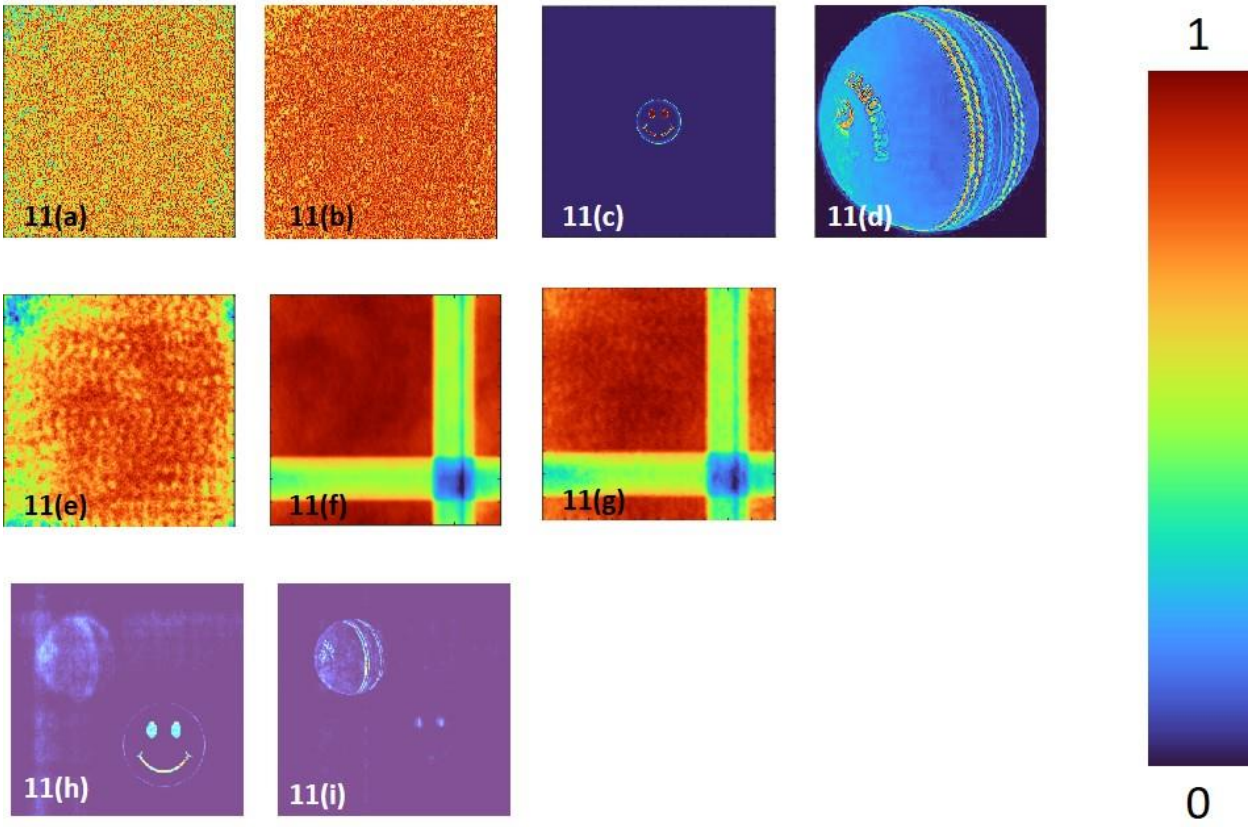

Figures 11(a) PSF1, 11(b) PSF2, 11(C) Object 1, 11(d) Object 2, 11(e) Intensity distribution of object 1, 11(f) Intensitydistribution of object 2, 11(g) Hologram, 11(h) Image reconstruction at plane 1, 11(i) Image reconstruction at plane 2

3. Software and Simulation

The image processing and image reconstruction was carried out using MATLAB. There are two steps namely hologram generation and hologram reconstruction. The procedure for hologram generation is as follows:

In line – 1, the matrix size was defined as N = 500 pixels. The PSF file was loaded into the system using the imread command in line – 2. A single channel of R, G and B was extracted for further processing in line – 3. In line – 4, the PSF matrix was resized to 500 x 500 pixels. In line – 5, the second PSF was synthesized by resizing the first PSF in 490 x 490 pixels. The matrix size was changed to 500 x 500 pixels using the padarray syntax in line - 6. Now the two PSFs corresponding to two depths or wavelengths is available. The test object is loaded next in line – 7. In line – 8, the test object's single channel was extracted. The image was then normalized in line – 9. The object was inverted to have a dark background in line – 10. The object was resized to 100 x 100 pixels in line 11. In lines 12 and 13, the image data was allocated to 201 to 300 pixels along the x and y directions of a matrix. In lines 14 and 15, the hologram was generated. This hologram can be generated either using one of the PSFs or formed by a summation of the holograms formed by two PSFs. In line 16, the generated hologram was displayed.

Step – 1 Hologram generation

Preprints (www.preprints.org) | NOT PEER-REVIEWED | Posted: 3 June 2022 doi:10.20944/preprints202206.0049.v1

```
Line – 1 N=500;
Line – 2 I=double(imread('file location'));
Line – 3 I1=I(:,:,1);
Line – 4 I1=imresize(I1,[500 500]);
Line – 5 I11=imresize(I2,[500*0.98 500*0.98]);
Line – 6 I11=padarray(I11,[5 5]);
Line – 7 A1=double(imread('file location'));
Line – 8 A1=A1(:,:,1);
Line – 9 A1=A1/max(max(A1));
Line – 10 A1=1-A1;
Line – 11 A2=imresize(A1,[100 100]);
Line – 12 A1=zeros(N,N);
Line – 13 A1(201:300,201:300)=A2;
Line – 14 Object=ifftshift(ifft2(fft2(I1).*fft2(A1)));
Line – 15 Hologram=Object.*conj(Object);
Line – 16 imagesc(Hologram)
```

The procedure for hologram reconstruction is as follows:

The Fourier transform was calculated for the hologram and the PSF using the syntax "(fftshift(fft2))" in Lines 17 and 18. The alpha and beta values were selected to tune the magnitudes of the above two matrices in lines 19 and 20. The non-linear reconstruction was applied in line 21. The intensity of reconstruction was calculated in line 22 and the reconstructed image was displayed in line 22 using imagesc syntax.

Step – 2 Hologram reconstruction

```
Line 17 R11=fftshift(fft2(I11));
Line 18 R22=fftshift(fft2(Hologram));
Line 19 alpha=0;
Line 20 beta=0.6;
Line 21 Recon_NLR=ifftshift(ifft2(((abs(R11).^alpha).*exp(1i*angle(R11))).*conj((abs(R22).^beta).*exp(1i*angle(R22)))));
Line 22 I=Recon_NLR.*conj(Recon_NLR);
Line 23 figure;imagesc(I)
```

4.Results and Conclusion

In this project, a proof-of-concept 3D imaging has been carried out with only two components and an overall cost of <10 USD for the entire project. The scattering lenses have higher speckle density and smaller speckle sizes in comparison to scattering glass plates. The semi-synthetic study yielded promising results. This project may lay foundation for the future manufacturing of low-cost 3D imaging systems.

Advisors:

Prof. Srinivasan, Prof. Dhanalakshmi, Prof. Vijayakumar Anand and Prof. Saulius Juodkazis.

Acknowledgement:
I would like to convey my genuine appreciation and profound gratitude to all my Advisors. I am highly obliged to **Prof. Srinivasan** (Head of the Department of Physics, Thiagarajar College, Madurai, Tamil Nadu, India) and **Prof. Dhanalakshmi** (Assistant Professor, Department of Physics Thiagarajar College, Madurai, Tamil Nadu, India) for their benevolent permission and approval to carry out this work in this institute. A special thanks to **Prof. Vijayakumar Anand** (ERA CIPHR chair and Associate Professor, Institute of Physics, University of Tartu, W. Ostwaldi 1 ,50411 Tartu, Estonia and Adjunct Associate Professor, Swinburne University of Technology, Australia) for giving me the opportunity to work on such an innovative project. Without his constant support and resourceful guidance, it was never been possible to possible to carry out this project work. My sincere thanks to **Prof. Saulius Juodkazis** (Tokyo Tech World Research Hub Initiative (WRHI), School of Materials and Chemical Technology, Tokyo Institute of Technology, 2-12-1, Ookayama, Meguro-Ku, Tokyo 152-8550, Japan and Optical Sciences Center and ARC Training Centre in Surface Engineering for Advanced Materials (SEAM), School of Science, Computing and Engineering Technologies, Optical Sciences Center, Swinburne University of Technology, Hawthorn, Melbourne, Victoria 3122, Australia) for his incredible support for this project. I owe my deep gratitude to **Mr. Aravind Simon** (Research Manager, ERA CIPHR Chair Institute of Physics, University of Tartu, W. Ostwaldi 1 ,50411 Tartu, Estonia) who took keen interest on my project work and guided me all along till the completion of my Project work by providing all the necessary information for developing a good system.

References

[1] Rosen, J., Vijayakumar, A., Kumar, M., Rai, M.R., Kelner, R., Kashter, Y., Bulbul, A. and Mukherjee, S., 2019. Recent advances in self-interference incoherent digital holography. *Advances in Optics and Photonics*, 11(1), pp.1-66.
[2] Zeng, T., Zhu, Y. and Lam, E.Y., 2021. Deep learning for digital holography: a review. *Optics Express*, *29*(24), pp.40572-40593.
[3] Smith, D., Ng, S.H., Han, M., Katkus, T., Anand, V., Glazebrook, K. and Juodkazis, S., 2021. Imaging with diffractive axicons rapidly milled on sapphire by femtosecond laser ablation. *Applied Physics B*, *127*(11), pp.1-11.
[4] Lin, X., Rivenson, Y., Yardimci, N.T., Veli, M., Luo, Y., Jarrahi, M. and Ozcan, A., 2018. All-optical machine learning using diffractive deep neural networks. *Science*, *361*(6406), pp.1004-1008.
[5] Vijayakumar, A. and Rosen, J., 2017. Spectrum and space resolved 4D imaging by coded aperture correlation holography (COACH) with diffractive objective lens. *Optics Letters*, *42*(5), pp.947-950.
[6] Antipa, N., Kuo, G., Heckel, R., Mildenhall, B., Bostan, E., Ng, R. and Waller, L., 2018. DiffuserCam: lensless single-exposure 3D imaging. *Optica*, *5*(1), pp.1-9.
[7] Anand, V., Ng, S.H., Maksimovic, J., Linklater, D., Katkus, T., Ivanova, E.P. and Juodkazis, S., 2020. Single shot multispectral multidimensional imaging using chaotic waves. *Scientific reports*, *10*(1), pp.1-13.
[8] Sahoo, S.K., Tang, D. and Dang, C., 2017. Single-shot multispectral imaging with a monochromatic camera. *Optica*, *4*(10), pp.1209-1213.
[9] Eils, R. and Athale, C., 2003. Computational imaging in cell biology. The Journal of cell biology, 161(3), pp.477-481.
[10] Coskun, A.F. and Ozcan, A., 2014. Computational imaging, sensing and diagnostics for global health applications. *Current opinion in biotechnology*, *25*, pp.8-16.
[11] Dicke, R.H., 1968. Scatter-hole cameras for x-rays and gamma rays. *The astrophysical journal*, *153*, p. L101.

 doi:10.20944/preprints202206.0049.v1

[12] Ables, J.G., 1968. Fourier transform photography: a new method for X-ray astronomy. *Publications of the Astronomical Society of Australia*, *1*(4), pp.172-173.

[13] Wagadarikar, A., John, R., Willett, R. and Brady, D., 2008. Single disperser design for coded aperture snapshot spectral imaging. *Applied optics*, *47*(10), pp.B44-B51.

[14] Chi, W. and George, N., 2011. Optical imaging with phase-coded aperture. *Optics express*, *19*(5), pp.4294-4300.

[15] Rai, M.R., Vijayakumar, A. and Rosen, J., 2018. Non-linear adaptive three-dimensional imaging with interferenceless coded aperture correlation holography (I-COACH). *Optics Express*, *26*(14), pp.18143-18154.

[16] Wan, Y., Liu, C., Ma, T. and Qin, Y., 2021. Incoherent coded aperture correlation holographic imaging with fast adaptive and noise-suppressed reconstruction. *Optics Express*, *29*(6), pp.8064-8075.

[17] Anand, V., Rosen, J. and Juodkazis, S., 2022. Review of engineering techniques in chaotic coded aperture imagers. *Light: Advanced Manufacturing*, *3*(1), pp.1-13.

[18] Rai, M.R., Vijayakumar, A., Ogura, Y. and Rosen, J., 2019. Resolution enhancement in nonlinear interferenceless COACH with point response of subdiffraction limit patterns. *Optics Express*, *27*(2), pp.391-403.

[19] Anand, V., Ng, S.H., Katkus, T. and Juodkazis, S., 2021. White light three-dimensional imaging using a quasi-random lens. *Optics Express*, *29*(10), pp.15551-15563.

[20] Wu, Y., Sharma, M.K. and Veeraraghavan, A., 2019. WISH: wavefront imaging sensor with high resolution. *Light: Science & Applications*, *8*(1), pp.1-10.